μ-SYNTHESIS CONTROL DESIGN APPLIED TO A HIGH SPEED MACHINING SPINDLE WITH ACTIVE MAGNETIC BEARINGS

Roger L. Fittro,[1] Carl R. Knospe[2]

ABSTRACT

Active magnetic bearings (AMBs) offer higher attainable surface speeds as well as other significant advantages in high speed machining (HSM) applications. In particular, dynamic compliance of the tool, which is directly related to machining performance, can be optimized via AMB feedback control design in a way that is not possible with conventional bearings. This paper deals with the design and implementation of a multivariable μ-synthesis controller for a 32000 rpm (3.48 million DN), 90 HP (67.1 kW) machining spindle. Careful attention is given to developing an accurate system model and an appropriate uncertainty description. In addition to the μ controller, an optimal decentralized PID controller is designed. Both theoretical and experimental results are presented, from which significant performance improvements are noticeable for the μ-synthesis control design.

1 INTRODUCTION

HSM spindles are specially designed to operate at cutting speeds well above that found in conventional spindles. Because machining spindles come in an assortment of sizes, it is common to categorize them on the basis of their operating surface speed (mm/sec) as opposed to rotational speed (rpm). The standard parameter used in the machine tool industry to measure surface speed is DN, which represents the bearing journal's outside diameter in millimeters multiplied by its rotational speed in rpm. Conventional spindles routinely operate in the range of 0 to 0.5 million DN. HSM spindles therefore encompass any spindle that operates well above this range.

For the production of any part in which machining makes up a significant percentage of the entire manufacturing process, increased machining speed can result in dramatic productivity improvements. This productivity improvement can result in more parts being made at a lower cost or allow the same machine to be used in the manufacturing of many different parts. Lower inventories associated with just-in-time manufacturing are also possible to maintain due to improved machining times. Furthermore, the productivity improvements associated

[1]Mechanical and Elect. Eng. Dept., Aston University, Aston Triangle, Birmingham B4 7ET, UK.
[2]Mech., Aerospace & Nuclear Eng. Dept., University of Virginia, Charlottesville, VA 22903, USA.

with HSM may make alternative component designs economically feasible and thereby open up the door to improved products without increased cost. In addition to improved productivity, research into high speed machining has shown that both tool temperature and the forces exerted on the cutting tool may decrease at higher speeds, both of which translate into improved tool life as well as enabling the manufacture of very thin walled parts.

The development of high-speed spindles has largely been dependent on improvements in rolling element bearing technology. Significant advancements have been made here, specifically the development of ceramic balls. However, further progress is hampered by the inherent limitations of these devices. The high centrifugal and cutting loads associated with HSM greatly limit the useful life of conventional bearings. To have acceptable life, bearing DN must be kept low, resulting in slender rotors which, in turn, have greater compliance and an increased tendency to chatter. In addition to short life spans, HSM operating conditions can cause ball bearing supported spindles to suffer catastrophic failure in the form of thermal lock-up (Stephens, 1995).

Because of the inherent limitations of rolling element bearings for high-speed spindles, research efforts have increasingly focused on alternate technologies. This paper examines the design and implementation of active magnetic bearings for high speed machining. There are two primary advantages to using active magnetic bearings in high speed machining applications. First, due to the noncontact nature of magnetic bearings, the maximum achievable surface speed is on the order of twice that of rolling element bearings. The second primary advantage is related to the tool's dynamic compliance transfer function. With standard bearing systems, this transfer function can only be slightly influenced during the bearing/spindle design procedure. With magnetic bearing systems however, this transfer function can be optimized to a much greater extent via the design of the AMB feedback control algorithm. Due to these two advantages, magnetic bearings possess the potential for achieving much greater performance and greatly advancing the capabilities of high speed machining.

2 ROBUST MULTIVARIABLE CONTROL

The performance objective of a HSM spindle is to achieve the maximum metal removal rate while maintaining acceptable machining accuracy for the manufacture of complex parts. From a machining spindle standpoint, maximizing the metal removal rate can be achieved via optimizing the spindle rotor geometry, rotational speed, and bearing placement and load capacity. All of these issues are addressed in detail in (Stephens, 1995). The requirement to maintain acceptable machining translates into two main performance goals: dynamic tool tip compliance minimization and chatter avoidance.

The primary force encountered in end milling operations corresponds to the cutting tool tooth pass frequency and its harmonics. However, since machining operations and cutting tools necessary to manufacture various parts, or even a single part, differ considerably, the force spectrum that a HSM milling spindle encounters is quite broad (Stephens, 1995). Therefore, it is necessary to design a HSM milling spindle which will have minimal tool tip deflection over a broad range of inputs with unknown spectra. This may be considered as a dynamic point compliance minimization problem. If the displacement of the tool tip in response to a force input at the tool due to the machining process is considered as a transfer function $\mathbf{T}_{xF}$, then the dynamic tool tip compliance minimization problem can be stated in mathematical terms as:

$$\min \left\| \mathbf{T}_{xF} \right\|_{\infty} \tag{1}$$

where $\|\cdot\|_{\infty}$ indicates the infinity norm of the transfer function. The chatter avoidance problem may also be cast as an infinity norm minimization problem (Stephens, 1995).

Because the two primary HSM milling spindle performance requirements may be cast as H_∞ minimization problems, AMB control system design via an H_∞-based control technique is considered in this paper. Although H_∞ control design theory offers very high performance potentials, standard H_∞ (without loop shaping) does not guarantee performance robustness. Since robustness is an essential characteristic for any practical control system design, a robust design procedure known as μ synthesis was used instead. μ Synthesis is a natural augmentation of H_∞ control theory with the analysis techniques of the structured singular value (Zhou, Doyle and Glover, 1996). It permits the design of multivariable controllers for complex linear systems with uncertainties in their model representations and guarantees system performance in the presence of these uncertainties.

3 EXPERIMENTAL SETUP

The prototype HSM spindle (see Figure 1) examined in this paper was designed to operate up to 32000 rpm (3.48 million DN). The spindle assembly consists of a 25.1 inch (638 mm) long shaft with a diameter that varies from 2.08 inches (52.8 mm) to 3.35 inches (85 mm). Inside the spindle shaft is a 25.7 in (652.8 mm) long, 0.56 in (14.22 mm) diameter drawbar which holds the various tools in place during cutting operations. Three cobalt iron laminated radial magnetic bearing journals are shrunk onto the outside of the shaft. These journals correspond to three magnetic bearing stators in the spindle housing. The first of these, the nose bearing, is located closest to the cutting tool and has a load capacity of 1200 lbf (5338 N). The second is located near the middle of the shaft, has a load capacity of 600 lbf (2669 N), and is referred to as the mid bearing. Finally, the tail bearing, also rated at 600 lbf (2669 N),

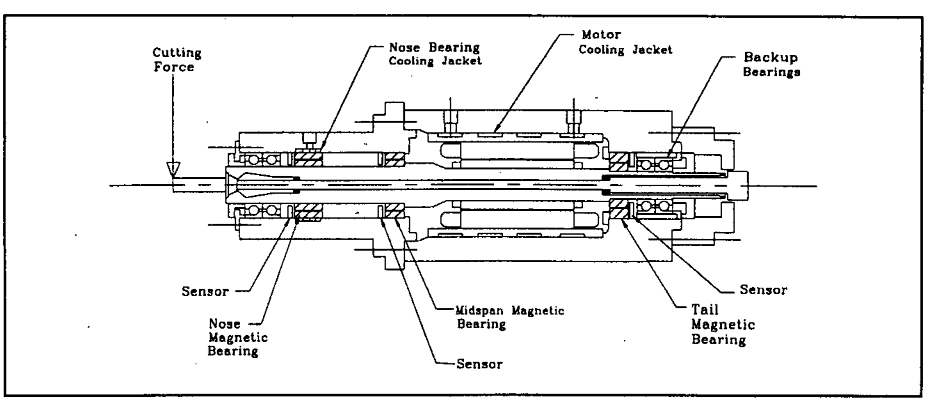

Figure 1: AMB HSM Spindle

is located toward the other extreme end of the shaft. The air gap for all three radial bearings is 0.0095 inches (0.241 mm). In addition to the journals, a magnetic bearing thrust disk and motor rotor are fitted to the shaft via interference fits. The thrust disk acts as the target for the magnetic bearing thrust actuators which are mounted to the spindle housing and have a load capacity of 1000 lbf (4448 N). The nominal thrust bearing air gap is 0.015 in (0.381 mm). The motor rotor is driven by a 3 phase AC induction motor rated for 40000 rpm and 90 HP (67.1 kW). Finally, the spindle assembly is fitted with optical sensors, next to each radial bearing, and two mechanical rolling element auxiliary bearings located at either end of the shaft. Completing the magnetic bearing control system are anti-aliasing filters, a parallel processing digital controller, and a bank of 150V, 15 A rms/30 A peak switching amplifiers.

4 MODELING

In order to develop high performance control system designs, very accurate models based on experimental data were first developed for all the HSM milling spindle components (see Figure 2). Once these models were developed, closed loop frequency response data was taken with the spindle in support under PID control and compared to that of the overall theoretical system model. Generally good agreement was found between the two. Although there were discrepancies between the theoretical closed loop model and the experimental data, these errors could all be connected to individual component modeling errors. These models were made as accurate as possible based on the given experimental testing procedures, consequently the discrepancies between the model and the actual spindle's frequency response were accounted for via uncertainty representations and the overall system description was deemed acceptable for control design synthesis.

5 UNCERTAINTY REPRESENTATION

Even though the rotor model was not perfect, no explicit uncertainty description was utilized for this component. Two standard uncertainty models have been traditionally used for structures: (1) unstructured additive uncertainty which is good for modeshape uncertainty; (2) highly structured uncertainty for natural frequencies and damping factors. The use of an additive uncertainty representation to cover unmodeled dynamics was deemed to be too conservative for the purposes of developing the desired high performance controller designs. Alternately, natural frequency uncertainties would require the addition of many repeated real uncertainty blocks, greatly complicating synthesis. A much simpler approach was used here. Uncertainty in the rotor model was handled implicitly through adding multiplicative uncertainty blocks to each actuator channel, which guarantee a certain multivariable gain and phase margin, and by allocating additional uncertainty to actuator open loop stiffness, K_x.

Appropriate uncertainty descriptions were developed based on the individual component modeling errors. The errors associated with the digital controller's zoh and delay, amplifier, and K_i were combined to form a single multiplicative uncertainty block in each input channel to the rotor model. This uncertainty was increased a further 5% as a measure to increase the input multivariable gain and phase margins. At the output side of the rotor, the sensor and

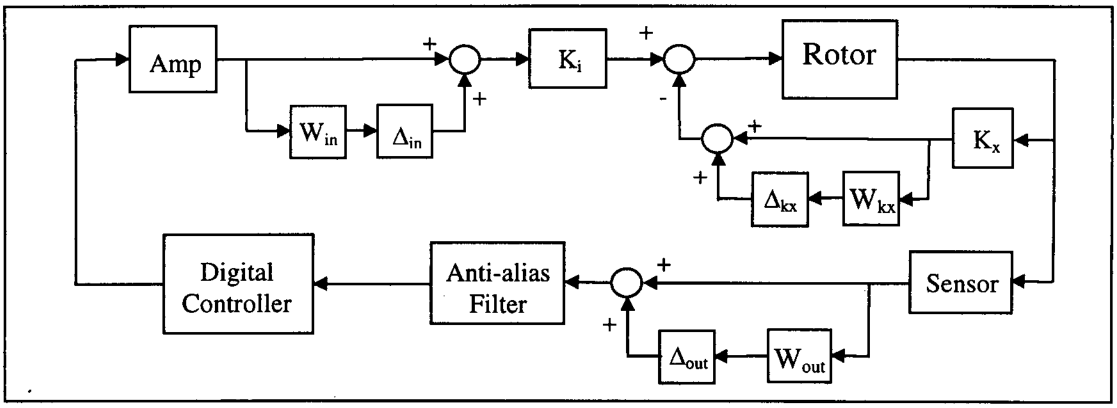

Figure 2: AMB HSM Spindle Block Diagram

anti-aliasing filter modeling errors were combined in a similar fashion to form a single multiplicative uncertainty block for each rotor model output channel. The sensor modeling errors were best represented by a constant percentage uncertainty while the size of the anti-aliasing modeling error was frequency dependent and determined to be best represented by:

$$W_{AA} = 0.04\frac{s + 0.1\omega_c}{s + 0.4\omega_c} \tag{2}$$

where ω_c is the anti-aliasing cut-off frequency in rad/sec. Finally, an uncertainty representation was included to account for the errors in the experimentally determined K_x values. The level of K_x uncertainty was also increased in order to enhance system robustness to small errors in the rotor natural frequencies. A summary of all of these uncertainty representations is shown in Table 1.

TABLE I: UNCERTAINTY REPRESENTATION

	Nose Bearing	Mid Bearing	Tail Bearing
Input Uncertainty	0.15	0.24	0.195
Output Uncertainty	0.02 + W_{AA}	0.02 + W_{AA}	0.03 + W_{AA}
K_x Uncertainty	0.10	0.15	0.15

6 PERFORMANCE SPECIFICATION

Dynamic tool tip compliance minimization was the only performance specification used for the development of the control system designs presented in this paper. When analyzed, the numerous cutting operations which make up the overall machining procedure can be translated into four different tool dynamic compliance specifications and associated frequency ranges (Stephens, 1995). These four categories are: 1) static compliance; 2) low frequency compliance; 3) medium frequency compliance; 4) high frequency compliance.

Static compliance corresponds to the positioning accuracy of the tool. With the use of an integrator in the magnetic bearing control design, static compliance can be made nearly zero up to the load capacity of the bearings. Low frequency tool tip compliance is an indication of the profiling accuracy of a spindle. The corresponding frequency range was determined by the acceleration of the spindle and the radius of curvature to be machined. For typical machining operations, these two parameters translate into a frequency range up to approximate 10 - 20 Hz. Tool compliance in the medium frequency range can be interpreted as the spindle's rough cut performance. This indicates how well the spindle removes large portions of metal while maintaining an acceptable surface finish. The medium frequency range corresponds to the tool toothpass frequency. For the HSM spindle operating with two or three tooth cutters, this frequency range is approximately 300 Hz to 1.6 kHz. Finally, high frequency tip compliance translates into the performance of a spindle in finishing operations. This performance specification can be taken to encompass frequencies above 1.6 kHz. Based on all of these cutting operations and associated frequency ranges, the following dynamic tool tip compliance weighting function was developed for use in control system design:

$$W_t = \frac{K_{W_t}(T_{n1}s+1)(T_{n2}s+1)}{(T_{d1}s+1)(T_{d2}s+1)} \qquad (3)$$

- allowed to be loosely controlled from 10-300 Hz

where: $T_{n1} = 1/(2\pi \cdot 10)$ $T_{n2} = 1/(2\pi \cdot 300)$
$T_{d1} = 1/(2\pi \cdot 2)$ $T_{d2} = 1/(2\pi \cdot 1200)$

and K_{Wt} is a scaling factor used during control design synthesis.

7 CONTROL DESIGN

An optimized PID controller was first developed for the HSM spindle as a benchmark. Because classical control design methods lack a formal optimization procedure, a PD controller was designed via an exhaustive search routine and then an integral term was added to this design in order to obtain nearly optimal static stiffness, while maintaining closed loop dynamic behavior at other frequencies. In addition to dynamic compliance performance, two other specifications were included in the PID control design procedure: 1) a fictitious pole was added to each channel of the plant in order to ensure a suitable phase margin for the closed loop system; 2) an asymmetric notch at the first bending mode was optionally included in the control design of the 3 bearings.

Next, a complex μ-synthesis control design was developed via MATLAB's Mutools toolbox *dkit* m-file. The uncertainty descriptions described in section 5 were utilized in this design procedure, and an appropriate controller gain and bandwidth limitation weighting function, W_c, was developed. Unlike the uncertainty weighting functions, it is not possible to accurately determine W_c prior to controller synthesis. Therefore, a practical controller weight, W_c, and optimal control design were determined in an iterative fashion as follows:

1) choose an initial guess for W_c
2) design an optimal μ controller (maximize K_{wt} such that $\mu \approx 1$)
3) implement
4) modify controller gain and bandwidth specification via W_c as appropriate

5) repeat steps 1) - 4) until the best practical control design is obtained

Using this procedure, a successful complex μ-synthesis controller was developed. Three D-K iterations were necessary to produce the final control design, which was comprised of 240 states and achieved a μ value of 1.02. Due to the large number of controller states, controller reduction was necessary before implementation was possible. Balanced model reduction was used to produce a reduced order controller and μ analysis was used to ensure stability and performance robustness. When combined, these two elements form an effective controller reduction method which guarantees closed loop system performance. Applying controller reduction to the 240-state μ control design, a 23rd order controller with an associated μ value of 1.04 was obtained.

8 THEORETICAL COMPARISON

The theoretical nominal dynamic tool tip compliances of the benchmark PID and μ controllers are shown in Figure 3. The maximum compliance of the nominal system with the μ controller is 58.54 μ-in/lbf (0.334 μm/N), approximately 22.4% better than that obtained with the optimal PID controller, 75.43 μ-in/lbf (0.431 μm/N). The best maximum compliance performance that can theoretically be achieved, as determined by H_∞ theory (Herzog and Bleuler, 1992), is 0.0 μ-in/lbf (0.0 μm/N). A control design which achieves this level of compliance is not practical however, as it requires nearly infinite gain and possesses no robustness. It does establish a fundamental limit on achievable performance though. The level of performance that could be achieved for the nominal system when the controller gain was limited in the same manner as in the robust μ controller was also examined (via μ synthesis). In this case, a peak compliance of 33.39 μ-in/lbf (0.191 μm/N) was achieved. In addition, a theoretical

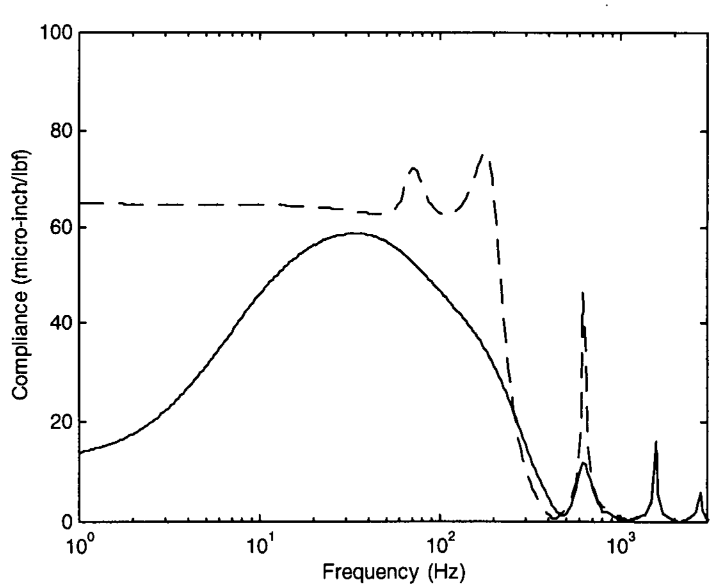

Figure 3: μ (solid) and PID (dashed) Nominal Compliance

high-gain μ control design was developed based on the same uncertainty description used for the robust μ controller, but without any control gain limitation imposed. This control design resulted in a maximum compliance of 13.77 μ-in/lbf (0.0787 μm/N). It is interesting to note the relationships between the nominal performance of the robust μ controller and these last two theoretical performance measures. The nominal performance of the μ controller is significantly greater than the limited effort optimal performance, which indicates that a significant degree of nominal performance is sacrificed to achieve the desired robustness. Even greater performance degradation is noticeable between the high-gain μ controller and the nominal μ design. These results indicate that both control effort and modeling uncertainty impose significant constraints on achievable compliance. Furthermore, the control effort limitation imposed on the μ controller appears to be a much stronger constraint than the given uncertainty description. Finally, it is interesting to compare the above performance figures to the static compliance achieved when the bearings are pinned (obtained with any PID control), 2.46 μ-in/lbf (0.014 μm/N).

Since the actual plant is never known perfectly, the experimental performance is likely to be worse for both controllers than these theoretical values for the nominal system. Therefore, a better comparison of performance of the two control designs is obtained by examining their worst-case compliance when the nominal model is perturbed. In this case, the μ controller significantly outperforms the optimal PID controller (see Figure 4). Worst-case compliance analysis applied to the PID control system resulted in a potential instability for the given uncertainty description. The μ-synthesis controller, on the other hand, has a predicted worst-case maximum point compliance of 74.47 μ-in/lbf (0.425 μm/N), which is actually slightly better than the nominal performance of the PID controller. In comparison, worst-case performance analysis of the closed loop system under optimal H_∞ and optimal μ control (control gain limitation but no uncertainty) resulted in possible instability, while the maximum predicted high-gain μ worst-case compliance was 16.17 μ-in/lbf (0.092 μm/N).

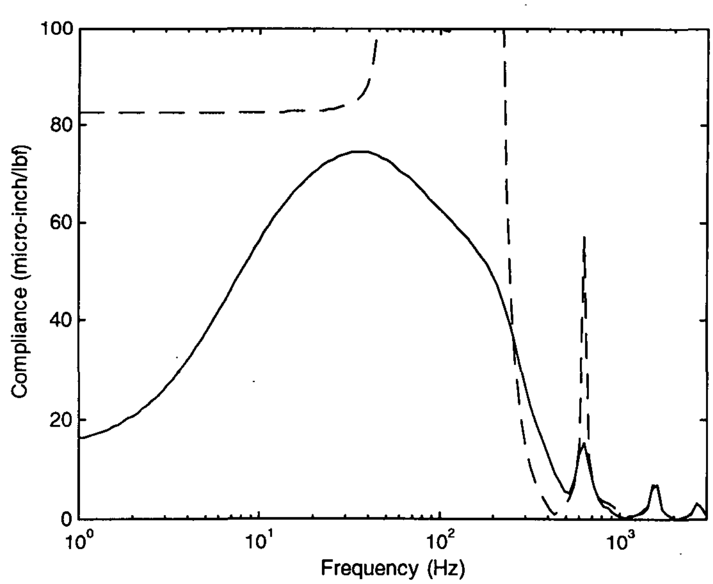

Figure 4: μ (solid) and PID (dashed) Worst-case Compliance

9 EXPERIMENTAL RESULTS

The controller used for implementation was a TMS320C40 DSP-based parallel processing digital controller designed and built at the University of Virginia (Fedigan et al., 1996). The control algorithm was programmed in assembly language in order to optimize its sampling rate capability for large order control designs. For the HSM spindle application, this allowed both the μ and PID control algorithms to be implemented at 12 kHz.

To determine the HSM spindle's dynamic tool tip compliance, impact tests were conducted. The tool was struck with an instrumented hammer and the resulting vibration was measured using a displacement sensor located at the tool tip. Figure 5 shows the tool tip compliance of the spindle with the benchmark PID controller. Also shown is the theoretical compliance determined from the system model. Figure 6 shows the experimental and theoretical compliances for the μ controller. For both controllers, especially the μ controller, there is a good agreement between theory and experiment (note that the magnitude scale is linear). The peak compliance for the μ controller is 56.53 μ-in/lbf (0.323 μm/N), a 41.7% improvement over that of the PID controller: 97.0 μ-in/lbf (0.554 μm/N). In addition, the significant performance improvements at low frequencies and at the first bending mode (600-700 Hz) should be noted. Clearly, the μ controller offers significant benefits in practice over the optimal PID control design.

Finally, robustness tests were conducted based on allowable tool mass variation, not an original performance design specification. Tests were run with no tool inserted in the spindle and with tools ranging from 0.50 inches (12.7 mm) in diameter and a weight of 2.20 lbf (9.79 N) up to 2.00 inches (50.8 mm) in diameter and a weight of 11.50 lbf (51.15 N). The μ controlled system remained stable for all but the largest tool configuration. This corresponds to a stability robustness of 8.22% with respect to the spindle's nominal weight of 60 lbf (266.9 N). The robustness of the spindle under PID control was not nearly as good. The PID

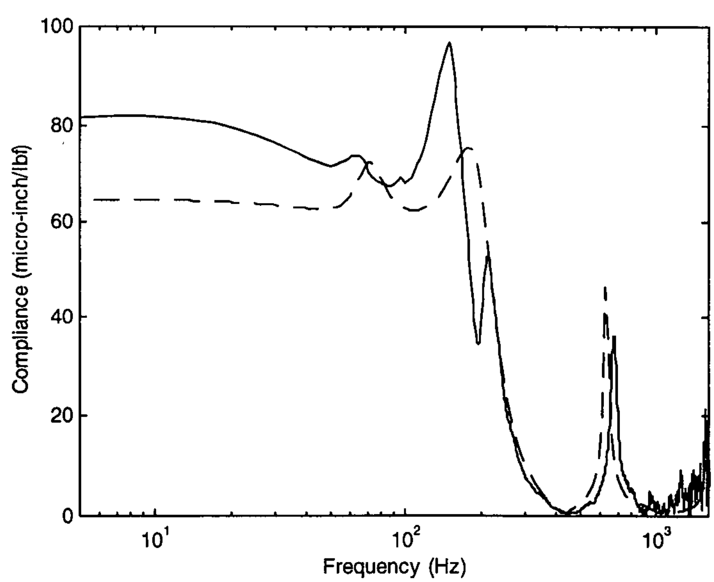

Figure 5: Experimental (solid) and Nominal (dashed) PID Compliance

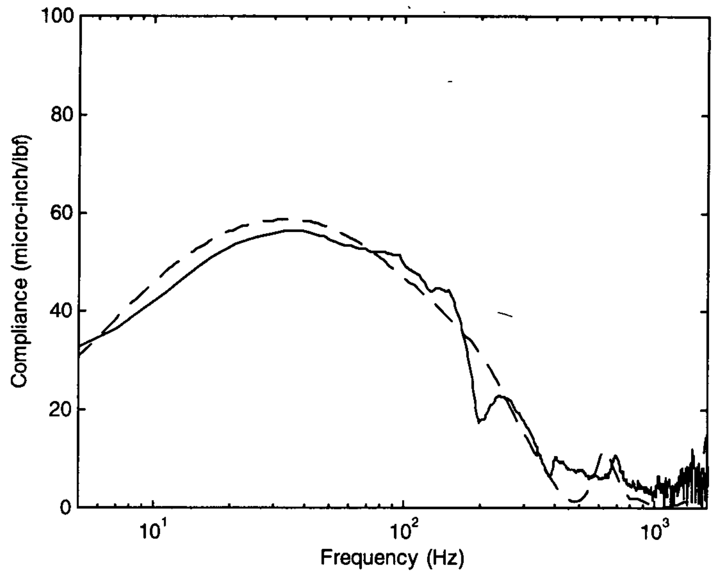

Figure 6: Experimental (solid) and Nominal (dashed) μ Compliance

controller resulted in an unstable system with no tool as well as with the smallest and largest tools. Therefore, the PID controller was only able to withstand a 3.24% spindle weight variation.

10 CONCLUSIONS

Optimal PID and μ-synthesis control designs were developed and implemented on a 32000-rpm (3.48 million DN) AMB HSM spindle. As the theoretical and experimental results presented demonstrate, μ synthesis can be employed to provide very good tool tip dynamic compliance. A significant improvement in performance was obtained over that of the optimal benchmark PID controller, while also achieving superior tool mass robustness.

REFERENCES

Fedigan, S.J., Williams, R.D., Shen, F., and Ross, R.A., "Design and Implementation of a Fault Tolerant Magnetic Bearing Controller", *Proceedings of the 5th International Symposium on Magnetic Bearings*, Kanazawa, Japan, August 1996, pp. 307-312.

Herzog, R. and Bleuler, H., "On Achievable H^∞ Disturbance Attenuation in AMB Control", *Proceedings of the 3rd International Symposium on Magnetic Bearings*, Alexandria, VA, July 1992, pp. 485-494.

Stephens, L.S., "Design and Control of Active Magnetic Bearings for a High Speed Machining Spindle", Ph.D. Dissertation, University of Virginia, August 1995.

Zhou, K., Doyle, J., and Glover, K., *Robust and Optimal Control*, Prentice Hall, Upper Saddle, NJ, 1996.